Sodium Channel Gating Currents in Frog Skeletal Muscle

DONALD T. CAMPBELL

From the Department of Physiology and Biophysics, University of Iowa, Iowa City, Iowa 52242

ABSTRACT Charge movements similar to those attributed to the sodium channel gating mechanism in nerve have been measured in frog skeletal muscle using the vaseline-gap voltage-clamp technique. The time course of gating currents elicited by moderate to strong depolarizations could be well fitted by the sum of two exponentials. The gating charge exhibits immobilization: at a holding potential of −90 mV the proportion of charge that returns after a depolarizing prepulse (OFF charge) decreases with the duration of the prepulse with a time course similar to inactivation of sodium currents measured in the same fiber at the same potential. OFF charge movements elicited by a return to more negative holding potentials of −120 or −150 mV show distinct fast and slow phases. At these holding potentials the total charge moved during both phases of the gating current is equal to the ON charge moved during the preceding prepulse. It is suggested that the slow component of OFF charge movement represents the slower return of charge "immobilized" during the prepulse. A slow mechanism of charge immobilization is also evident: the maximum charge moved for a strong depolarization is approximately doubled by changing the holding potential from −90 to −150 mV. Although they are larger in magnitude for a −150-mV holding potential, the gating currents elicited by steps to a given potential have similar kinetics whether the holding potential is −90 or −150 mV.

INTRODUCTION

Small, rapid, asymmetric charge movements attributed to the sodium channel gating mechanism have been measured and extensively characterized in invertebrate giant axons and frog myelinated nerve (reviewed by Armstrong, 1981). Similar fast asymmetric currents have been described in frog muscle in several preliminary reports (Vergara and Cahalan, 1978; Rojas and Suarez-Isla, 1980; Campbell, 1981; Hahin and Campbell, 1982; Sizto, 1982) and one longer study (Collins et al., 1982*b*). In intact muscle these sodium channel gating currents are accompanied by larger and slower charge movements thought to be involved in excitation-contraction (E-C) coupling, which have been studied extensively (Schneider and Chandler, 1973; Chandler et al., 1976; Horowicz and Schneider, 1981). The purpose of this paper is to establish the basic characteristics of the fast asymmetric current in frog

J. GEN. PHYSIOL. © The Rockefeller University Press · 0022-1295/83/11/0679/23 $1.00

Volume 82 November 1983 679–701

muscle for comparison with previous work in nerve. An important secondary goal is the demonstration that gating currents can be measured in skeletal muscle with high resolution and without significant contamination from the slower E-C coupling charge movements.

In this paper, the fast charge movement will frequently be referred to as the "gating current," although so far no unequivocal method has been devised in this or in any other preparation for separating true sodium channel gating current from possible contamination by asymmetric charge movements of other origin. Although many of the results are similar to those previously reported by Collins et al. (1982*b*), the methods used here have provided additional resolution at early times. This has permitted a better estimate of total charge at the ON and OFF of voltage steps.

METHODS

The vaseline-gap voltage-clamp technique (Hille and Campbell, 1976) was used to study single skeletal muscle fibers from the semitendinosis muscle of either northern *Rana pipiens* or *Rana catesbeiana*. Pieces of single muscle fibers are dissected free from the body of the muscle in normal Ringer solution (in mM: 115 NaCl, 4 KCl, 2 $CaCl_2$, and 4 HEPES at pH 7.4) and transferred to the recording chamber containing CsF solution. In freshly dissected fibers the CsF solution causes the fiber to shorten (Hille and Campbell, 1976). This shortening can be taken as a sign of health, since damaged (and therefore depolarized) regions of the fiber are identifiable by their failure to shorten. Shortening can be prevented by holding the fiber slightly stretched and depolarizing it slowly by gradually changing the bathing solution from Ringer to CsF. No difference in sodium or gating currents has been detected between shortened and rest-length fibers. However, shortening increases the fiber diameter, which by decreasing the axial resistance permits a slightly higher-frequency response of the voltage clamp. Seals of vaseline or vaseline plus vacuum grease are applied across partitions separating the four pools. The ends of the fibers are cut near the outside seals. After connecting the chamber to the electronic apparatus with combination agar-bridge/Ag-AgCl electrodes, K-free Ringer is washed into the pool containing the artificial node ("pool A," using the nomenclature of Hille and Campbell [1976], which is in turn derived from Dodge and Frankenhauser [1959]).

After the wash-in of Ringer, the preparation is cooled and allowed to "settle in" for 30–45 min before gating current measurements are initiated. The settling-in period serves several purposes. First, it permits the CsF to diffuse from the cut ends into the fiber where the F^- prevents the Ca concentration from reaching the contraction threshold. Second, the vaseline tends to seal more tightly to the fiber during this period. Third, during the first 15–30 min after the wash-in of Ringer, the bulk of the slowly charging component of fiber capacitance, which presumably arises from the transverse tubular system (T system), is lost. This electrical uncoupling of the T system is important because it minimizes the contribution of gating currents arising from Na channels within the T system that are expected to have kinetics distorted by the delay of tubular charging. This phenomenon has been described briefly (Campbell and Hahin, 1983) and will be treated at length in a later paper (D. T. Campbell and R. Hahin, manuscript in preparation).

The K-free Ringer contains 115 mM NaCl, 2 mM $CaCl_2$, and 5 HEPES at pH 7.4. CsF solutions used for the end pools contain either 120 mM CsF or 115 mM CsF plus 5 mM NaF, buffered with 3 mM HEPES at pH 7.3. The gating current solution

consists of 115 mM tetraethylammonium bromide, 5 mM CsCl, 2 mM $CaCl_2$, and 4 mM HEPES titrated to pH 7.4 with *N*-tris-(hydroxymethyl)aminomethane base (Tris) and 10^{-6} M tetrodotoxin (TTX) to block sodium currents. The absence of K and the small amount of Cs used in the gating current solution seemed to increase the linearity of the leakage current, although this was not studied in detail.

With the vaseline-gap technique, membrane potential is measured indirectly: the fiber interior is held at virtual ground potential by a feedback amplifier and membrane voltage is measured as the negative of the voltage in pool A. In one change from the original method, the amplifiers used to measure this potential were zeroed independently using passive components and it was assumed that this balance then provided an accurate measure of the membrane potential. Since a variety of causes can contribute errors to this measurement, an independent measure of voltage is desirable. For this purpose, the steady state inactivation vs. voltage relationship is determined at the beginning of experiments and preparations are discarded if the midpoint of this relationship is shifted >5 mV from the average value of −75 mV. Junction potentials of the solutions used are <1 mV and no correction for these is applied.

Current is measured with a current-to-voltage converter, rather than being measured as a voltage drop across the axial impedance, Z_{ED} (from one cut end of the fiber to the region inside the cell in pool A). Series resistance is minimized by using separate agar-bridge/Ag-AgCl electrodes in pool A for current passing and voltage measuring. Residual resistance in series with the surface membrane is measured from the "hop" of voltage in response to a current-clamp step. It is in the range 0.5–1.5 Ω cm^2 (1–3 Ω μF^2) and is compensated for electronically. Judging from the ~3–4-ms time constant of charging of the residual T system capacitance, a larger resistance is in series with it. This series resistance is not compensated, and thus any Na channels in this tubular membrane might be expected to contaminate surface membrane charge movements. However, because of the delays in charging the tubular membrane, this charge would move 10–40 times more slowly than surface gating currents (see gating current time constants in Fig. 14), and therefore the amplitude of its asymmetry current would be attenuated by ~1/10–1/40 of the amplitude it would have if it were located on the surface. Such a small, slow current is unlikely to be resolved in the 1–4-ms integration interval of the present experiments. In support of this notion is the observation that no difference is seen between charge movements from fibers with a 96% loss of T system capacitance and those with a more moderate loss of 70–80% of the T system capacitance.

A transient generator driven by the voltage-clamp command signal is used to electronically subtract the bulk of the linear capacity and leakage currents (Armstrong and Hille, 1972; Hille and Campbell, 1976). Residual linear currents are subtracted digitally as described below. The signal from the transient generator is subtracted from the membrane current at a differential amplifier, filtered at 30–50 kHz by a four-pole Bessel filter, amplified 20–100 times, and filtered again at the same cut-off frequency by another four-pole Bessel filter. This filtration slows the 10–90% rise time of the current-measuring response to 14–22 ms. The filtered and amplified current signal is sampled by a 12-bit A-D converter (Data Translation, Natick, MA) at two different sample intervals: 10-μs intervals are used at early times during the rapid phase of gating current, and 20-, 50-, or 100-μs intervals are used at later times. This procedure permits good time resolution to be obtained using 256 samples per record. These records are transferred from the memory of the computer (PDP 11/03; Digital Equipment Corp., Marlboro, MA) onto floppy diskettes for later analysis.

Four to six control steps, typically 30-mV depolarizations, are made from a base potential of −180 mV. These are followed by 4–12 test steps of increasing amplitude from the holding potential. The currents elicited by the control steps are summed and then scaled appropriately before subtracting them from each of the test currents. The result of this procedure represents the nonlinear portion of the membrane current (Schneider and Chandler, 1973; Armstrong and Bezanilla, 1974). In practice, a sequence of control and test steps is repeated 8–64 times and the currents are averaged in order to increase the signal-to-noise ratio. Control steps are confined to a voltage range where nonlinear current was found to be absent (see Fig. 3). Both control and test steps are rectangular (the step up to the test or control potential is equal to the step down). In contrast to more complicated pulse shapes, this permits the identical control records to be used with each of the test currents. This ensures

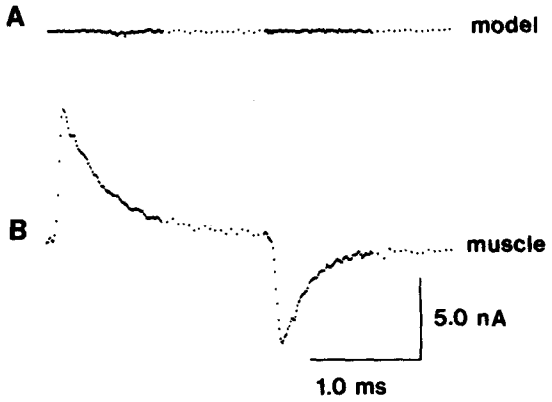

FIGURE 1. Linearity of the apparatus. (*A*) A two-time-constant model of the muscle preparation was connected to the electronic apparatus used in the gating current experiments and a gating current pulse protocol was applied. The response to a 90-mV test potential is shown. As in the muscle experiments, the bulk of the linear leakage and capacity current is subtracted using a combination of analog and digital methods described in the text. The current is the average of 64 test steps, filtered at 50 kHz before digitization. Very little nonlinear current is evident after the subtraction procedure. (*B*) The response of a muscle fiber to the same pulse protocol applied in *A* is shown at the same gain.

that kinetic differences observed at different test potentials are not a consequence of differences in the control pulses. In addition, because separate control traces are not required for each test pulse, this protocol saves time over the more standard P/4 or equal-and-opposite pulse protocols.

A run consisting of 32 sweeps of a pulse sequence takes 4–9 min. In the medium term (15–30 min), successive runs in the same solution typically show no alteration of kinetics or maximum charge. However, over the 2–3-h course of an experiment, it is typical for the total charge to decrease by 5–15% with no apparent change in kinetics. Some of this change appears to be correlated with slight flowing of the seals and is minimized at lower temperatures. The remainder may reflect fiber "rundown."

Measurement of gating currents makes stringent demands on the electronic apparatus because any nonlinearities in the apparatus would contribute artifactual current to the measured asymmetric charge movement. Fig. 1*A* shows a test of the circuit linearity. When a linear electrical model of the muscle preparation is connected

to the apparatus, stimulation with a standard gating current pulse protocol elicits virtually no nonlinear charge movement. By contrast, Fig. 1*B* shows the gating current that results when the same 90-mV test pulse is applied to a muscle fiber. These results support the conclusion that the nonlinear current observed in Fig. 1*B* arises from nonlinearities in the muscle membrane and not from the apparatus. To achieve the linearity illustrated in Fig. 1*A*, the frequency and gain characteristics of the various stages of the voltage clamp, transient generator, and recording system were carefully adjusted. The strategy used was to tailor the signal and the amplifiers at each stage so that no amplifier was allowed to saturate or to be "slew-rate limited" during voltage transitions. The use of the analog transient generator to accomplish the initial subtraction of linear capacity and leakage currents permits substantial amplification of the current signal before digital sampling without causing saturation of the A-D converter (Armstrong and Bezanilla, 1977). In turn, this minimizes the digitization error that would otherwise occur at lower gains.

A frequently applied alternative to the above approach is to "blank" the current signal for a short time immediately after a voltage transition. Fig. 2 shows the effect of such a procedure and emphasizes the importance of linearizing the electronic apparatus. Fig. 2*A* shows a family of gating currents recorded for depolarizing steps (ON gating currents) at a temperature of 12.4°C. The dotted line is drawn 50 μs after the test step and illustrates the consequence of using a 50-μs blanking interval. Fig. 2*B* shows the integral of the gating current for a step to +30 mV. It demonstrates that although at 50 μs the current is still close to its peak value, nonetheless, over 30% of the charge has moved by this time. Because the kinetics of charge movement are voltage dependent, the amount of charge lost by this procedure is also voltage dependent, with a minimum at about −30 mV, where the charge movement is slowest. In the experiment illustrated in Fig. 2*A*, the use of a 50-μs blanking interval would have caused an average loss of 25% of the gating charge measured for depolarizations between −90 and +30 mV. Even at lower temperatures, where the charge movement is slowed, the loss is significant. Thus, in another fiber studied at 8°C with test potentials between −60 and +60 mV, a 30-μs blanking period caused an average 8% loss of charge, and increasing the blanking interval to 40, 50, 60, and 70 μs resulted in average losses of 15, 23, 28, and 33% respectively.

Integration of Gating Current

Because the gating current transient rarely settles to the zero-current level, integration of the record requires that a suitable baseline for the integration be chosen. Fig. 3 illustrates the two methods that have been used. In general, the horizontal-baseline method shown in Fig. 3*A* was applied. The sloping-baseline method shown in Fig. 3*B* was used when the pedestal was so steep that the two methods gave significantly different results. Even in the fibers that exhibited them, such sloping pedestals were only apparent for the strongest depolarizations (beyond about +30 mV). The integration intervals ranged from ~4 ms for the slowest moving charge at temperatures of 4–5°C, to ~1.5 ms for the rapidly moving charge elicited by steps to +60 mV at 15°C.

RESULTS

Negligible Charge Moves at Potentials Below −135 mV

The procedure used to measure gating current assumes that nonlinear currents are absent over the range of voltages used for measuring the control

currents. Fig. 4 shows a test of this assumption. In this experiment the muscle fiber was held at −165 mV and the control pulse was a 15-mV depolarization from a base potential of −180 mV. Upon subtracting the appropriately scaled control currents, test steps from −165 to −158 and −143 mV elicited negligible charge movement. That is, the currents elicited by steps to −158 and −143 mV are linearly proportional to the control currents measured in

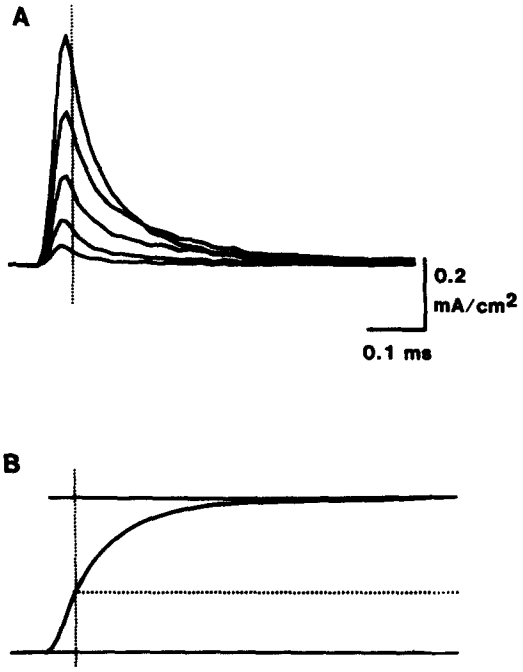

FIGURE 2. The effect of a 50-μs "blanking" interval. (*A*) A family of muscle gating currents recorded for steps to between −90 (bottom) and +30 mV (top) from a holding potential of −150 mV. The dotted line is drawn 50 μs after the step in voltage after accounting for the delay introduced by the eight-pole, 31-kHz Bessel filter. (*B*) The integral of the top (+30 mV) record displayed at the same time scale. The total charge represented by the upper horizontal line was 24.0 pC. As in *A*, the vertical dotted line is drawn 50 μs after the voltage step. The horizontal dotted line represents the charge moved during the 50-μs interval, ~35% of the total charge at this voltage. Muscle 213, temperature 15°C.

steps from −180 to −165 mV. A step to −128 mV elicited the movement of 0.37 pC of gating charge, equal to 1.5% of the peak charge (24.9 pC) that was measured in a step from −165 to +45 mV. In most of the experiments described below the control pulses were 30-mV depolarizations from a base potential of −180 mV, and thus control currents are expected to contain negligible nonlinear charge movement. In a few early experiments the control steps were depolarizations from −180 to −120 mV, in which case the total

charge for strong depolarizations would be underestimated by ~5% because of the nonlinear charge that moves between about −135 and −120 mV.

A Variety of Nonlinear Currents Are Measured in Muscle

Fig. 5 shows charge movements recorded for steps to 0 and +60 mV and displayed at two very different time scales. In *A*, rapidly moving gating current transients elicited by 3-ms depolarizations are seen. For a test pulse

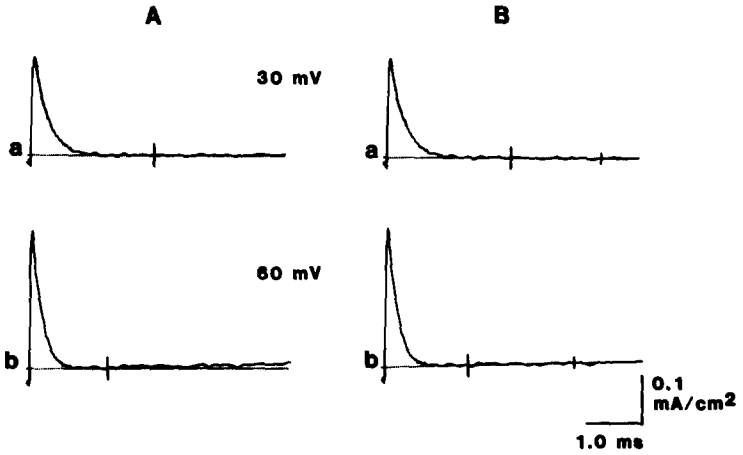

FIGURE 3. Integration of the gating current records. Gating currents elicited by steps to +30 and +60 mV from a holding potential of −150 mV. (*A*) Integration using a horizontal baseline is illustrated. A cursor is positioned beyond the point where the current transient has settled, and 5–20 data points centered on the cursor are averaged. The current above this baseline is then integrated, beginning with the onset of the test pulse and ending at the cursor. In *A* (*a*), the integration interval is 2.5 ms, and the charge was 24.2 pC. Changing this interval to 2, 3, or 4 ms did not significantly change the calculated charge because the pedestal is nearly flat over this time range. *A* (*b*) illustrates the horizontal baseline method applied to a gating current transient, which exhibits a sloping pedestal. In this case, the cursor is positioned at the local minimum of current for an integration interval of 1.4 ms, yielding a charge of 24.6 pC. (*B*) The same current records shown in *A* are shown analyzed using a sloping baseline fitted between the two cursors. The current above this line is integrated from the onset of the pulse up to the larger cursor. Using this method, the integral in *B* (*a*) was 24.3 pC, and in *B* (*b*) it was 25.2 pC.

to +60 mV, the early gating current transient is followed by a slowly rising outward current pedestal. Fig. 5*B* shows currents measured in the same fiber using 80-ms test pulses to the same two voltages and displayed at the same gain (the early gating current transients in *B* are attenuated by the lower cut-off frequency of the electronic filter). The records in Fig. 5*B* illustrate that what appear to be relatively simple pedestals in *A* have a more complicated time course. The middle "bump" of current seen at +60 mV has a shape

which suggests that it may be the slow charge movement that has been linked with the process of E-C coupling in skeletal muscle (Schneider and Chandler, 1973). For the step to 0 mV this slow charge movement is smaller and results in less total charge moved than the step to +60 mV. By contrast, the slow charge movement in intact frog muscle saturates at ~0 mV. In this and one other fiber in which it was found, the kinetics and the steady state distribution of this slow charge appear to be shifted 20–30 mV in the depolarizing direction relative to the slow charge measured in intact muscle. The long ON pulses of Fig. 5*B* are followed by large inward charge movements not seen in *A*. Apparently, very little of the slow charge moves outward during the 3-ms

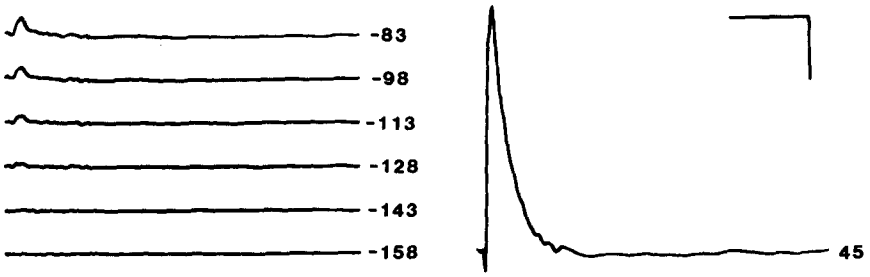

FIGURE 4. Charge movement at hyperpolarized potentials. Left: To determine the extent of charge movement at very negative potentials, the fiber was held at −165 mV and stepped to potentials between −158 and −83 mV. Currents are the average of 32 sweeps of a pulse sequence consisting of 10 control steps from −180 to −165 mV, followed by the six test pulses. Additional digital smoothing equivalent to a filter bandwidth of 25 kHz (Hamming, 1977) was applied to the data to facilitate visualization of the gating current. The gating charge at −158 mV is negligible. The charge moved at −143, −128, −113, −98, and −83 mV was 0.18, 0.37, 0.63, 0.91, and 1.94 pC, respectively. Right: Shown for comparison at the same gain is the gating current measured in the same fiber for a step to +45 mV from a holding potential of −165 mV. A charge of 25.0 pC was carried by this current transient. Thus, the nonlinear charge that moves between −165 and −143 mV is <1% of the maximum charge moved for a large depolarization. Horizontal calibration is 0.5 ms, vertical calibration is 0.1 mA/cm^2. Muscle 234, temperature 8°C.

pulses used in Fig. 5*A*, and that part which does recovers too slowly during the OFF step to −90 mV to be resolved as anything other than a small, relatively flat pedestal. After the peak and decline of this slow charge movement at +60 mV, the outward current increases again at late times. The origin of this late outward current is not known, but it may represent ionic current, possibly passing through delayed rectifier channels that are blocked by Cs at more negative potentials.

Long-duration test pulses like those used to elicit the slow charge movements in Fig. 5*B* were used in eight experiments. Significant slow charge movement was seen in only two experiments and only when the measurement was made before the customary settling-in period. (The currents shown in

Fig. 5*A* were recorded ~12 min after the start of the experiment and the currents recorded in Fig. 5*B* were recorded ~4 min later.) In the other fiber (not shown), slow charge movements seen early in the experiment were absent in traces recorded ~30 min later. Fig. 6 illustrates the more common finding. Again, two sets of records from a single fiber are displayed at the same gain and on very different time scales. In *B*, the early outward gating current is greatly attenuated by the 1-kHz filter frequency used. The outward "bump" of current seen in Fig. 5 is absent. At +30 mV the pedestal is nearly

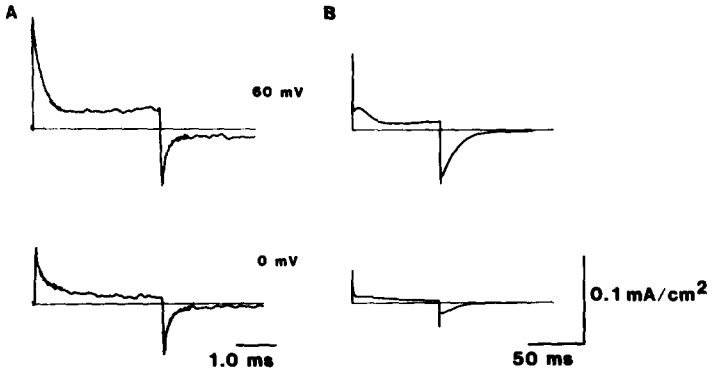

FIGURE 5. Fast and slow charge movements in muscle. (*A*) Gating currents recorded for 3-ms steps to 0 and +60 mV from a holding potential of −90 mV. Signals were electronically filtered at 50 kHz and averaged for 32 pulse sequences. (*B*) Slow charge movements, recorded in response to an 80-ms pulse in the same fiber, are illustrated at the same gain. The currents were electronically filtered at 10 kHz and averaged for eight pulse sequences. The stronger filtering has blunted the fast gating current. In this and in one other fiber studied with long voltage pulses, the pedestal of current seen at strong depolarizations has a complicated time course resembling the slow charge movement that has been attributed to the process of excitation-contraction coupling. In both fibers the kinetics of the slow charge movement appeared to be slowed and the steady state distribution of the slow charge shifted in the depolarizing direction compared with microelectrode recordings made from intact muscle (Chandler et al., 1976) and single-gap voltage-clamp recordings made from rest-length fibers cut in a solution of Cs glutamate, EGTA, Mg, and ATP (Horowicz and Schneider, 1981). Muscle 94, temperature 4.1–4.2°C.

flat, whereas at +60 mV the outward current increases slowly with time. Current pedestals are typically smaller than those in the records of Figs. 5 and 6 (for example, Fig. 9*A*) and many fibers exhibit virtually no pedestal at all (for example, Fig. 2).

Immobilization of Gating Charge

For a fiber held at −90 mV, the quantity of charge that moves during the inward gating current transient after the return to the holding potential

depends on the voltage and duration of the preceding step. For any particular ON voltage the charge following the step (the OFF charge) first increases and then decreases as the duration of the prepulse is increased (Armstrong and Bezanilla, 1977). Fig. 7 shows the ratio of the OFF charge to the ON charge that moved during prepulses to −30 (*A*) and 0 mV (*B*). This ratio is near unity for short-duration prepulses and declines to ~0.3 for longer durations. This is similar to the decline reported in squid axon that has been called "charge immobilization." As in the squid axon, charge immobilization parallels the inactivation of the sodium current. The curves in Fig. 7 are exponentials that decline from 1.0 to 0.3 with time constants equal to τ_h determined from ionic currents measured at the same voltages in the same fiber. Although there is not sufficient precision in the gating current data to constrain the

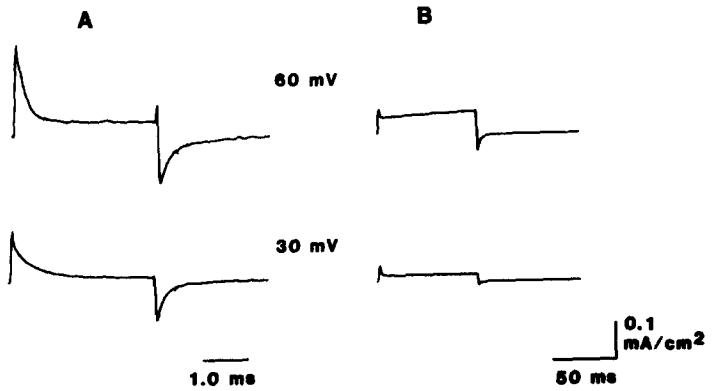

FIGURE 6. Late currents measured in a cut muscle fiber. As in Fig. 5, gating currents elicited by 3-ms test pulses are compared with currents recorded with 80-ms depolarizations to the same potentials. (*A*) Gating currents measured with electronic filtering at 50 kHz. (*B*) Late current measured in the same fiber displayed at the same gain but filtered at 1 kHz. In *A* the gating current measured at +30 mV has a slight outward current pedestal, which in *B* is seen to be nearly flat over the 80-ms step. The larger pedestal seen for a step to +60 mV is seen in *B* to rise slowly at late times. There is no evidence of the transient slow charge movement seen in Fig. 5. Muscle 90, temperature 4.2°C.

fits independently, the τ_h curves approximate the time course of charge immobilization and support the notion that immobilization reflects the inactivation of ionic current.

OFF Charge at Hyperpolarized Holding Potentials

One criterion for gating charge established early in the development of the gating current hypothesis is that it should be "capacitative." That is, for gating current to represent the movement of channel structures integral to the membrane, this movement should be confined to the membrane. In turn, this means that the amount of charge moved during the ON pulse should be equal to the charge that returns during the OFF pulse. This concept is complicated by the observation of charge immobilization as discussed above.

Armstrong and Bezanilla (1977) demonstrated that the apparent loss of OFF charge was actually an inability to resolve it during its slow return. They found, however, that returning the membrane to hyperpolarized potentials speeded the return of immobilized charge and thereby allowed its movement to be detected as a slow transient in the OFF gating current. Fig. 8*A* illustrates this effect in frog muscle. Superimposed and scaled so that the peak inward currents are approximately the same size are two OFF gating current transients recorded upon returning to −120 mV from 0.3- and 5-ms prepulses to +30 mV. Both transients exhibit rapid and slow phases in the decline of current, although the proportion of charge in the slow phase is considerably larger after the 5-ms prepulse. For both durations of prepulse, the sum of the fast and slow components of OFF charge is approximately equal to the charge

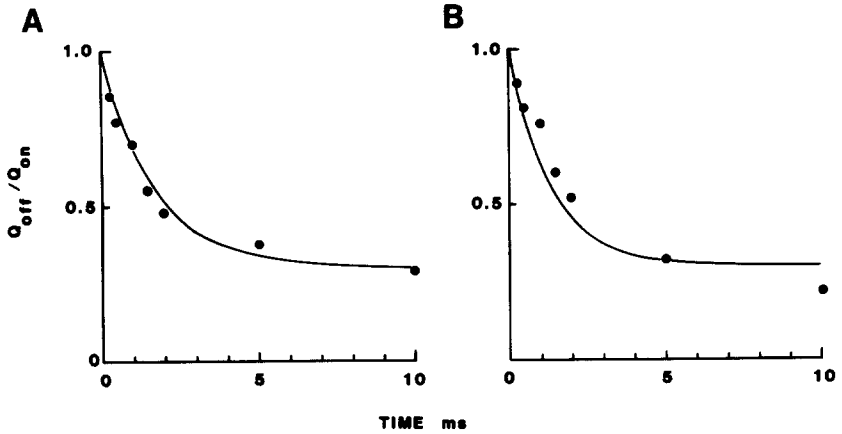

FIGURE 7. Immobilization of gating charge. The ratio of OFF charge measured for a return to the holding potential of −90 mV to the ON charge moved during the prepulse is plotted against prepulse duration. The curves are single-exponential decays from 1.0 to 0.3 that have the time constants of inactivation determined from fits to the falling phase of ionic current measured earlier in the same fiber at the same voltages. (*A*) Test pulse −30 mV, time constant 1.7 ms. (*B*) Test pulse 0 mV, time constant 1.3 ms. Muscle 26, temperature 4.2°C.

moved during the preceding ON pulse. These results are consistent with those of Fig. 7 and suggest that the charge immobilized during a depolarizing step returns quickly enough at −120 mV to be resolved.

Fig. 8*B* demonstrates that the size of the slow component of gating current increases with increasing prepulse amplitude. ON and OFF gating currents are displayed at the same gain. The 0.5-ms prepulse to −30 mV elicits an OFF gating current with virtually no slow component, whereas the +30-mV prepulse results in an OFF current with a considerable slow phase.

Interpretation of the slow OFF transient as recovery from immobilization is supported by the records illustrated in Fig. 9. Fig. 9*A* shows ON and OFF gating current transients elicited by potential steps spaced 30 mV apart, from a holding potential of −150 mV. Plotted in Fig. 9*B* is the charge moved

during the ON pulse vs. the total charge (the sum of both the fast and slow phases) moved during the corresponding OFF pulse. The line is drawn with a slope of 1 and an intercept of 0. A linear regression of the points yields a slope of 1.00 and an intercept of 1.01 pC, with a correlation coefficient of .99. A simple interpretation of this result is that virtually all of the ON charge returns quickly enough to be measured upon repolarization to −150 mV.

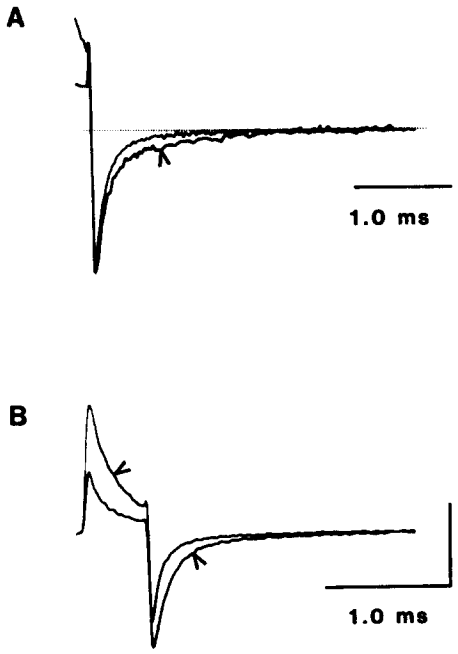

FIGURE 8. Slow transients of OFF gating current. (*A*) OFF-gating current transients at −120 mV in response to +30-mV prepulses 0.3 and 5 ms in duration. For the sake of comparison, the currents have been scaled so that the peaks approximately coincide. After the 5-ms prepulse, a large slow component of OFF gating current is seen (arrow). The amount of slowly moving charge in each record was estimated from a single-exponential fit to the slow component. After the 0.3-ms prepulse, the slow component accounted for 26% (4.22 pC) of the 16.31 pC of charge moved, whereas after the 5-ms prepulse, the slow component accounted for 69% (18.7 pC) of the 27.1 pC of charge moved. (*B*) ON and OFF gating current transients superimposed at the same gain for 0.5-ms prepulses to −30 and +30 mV. For a fixed duration prepulse, the slow component of charge increases with the prepulse amplitude. Muscle 181, temperature 4.3°C.

This near-equality of ON and OFF charges is also obtained at potentials above +30 mV, which supports the idea that the pedestals described above do not seriously interfere with the integration of charge.

Steady State Distribution of Charge

Several methods have been used previously to determine a steady state charge

vs. voltage relationship. A common method, that of measuring gating charge using only depolarizating steps from a moderate holding potential of −70 or −90 mV, ignores the charge that moves at more negative voltages. This charge is illustrated in the inset to Fig. 10, which shows the asymmetric current elicited by a step from −90 to −150 mV. This current transient, recorded at 5°C, exhibits two distinct phases that can be well fitted by the

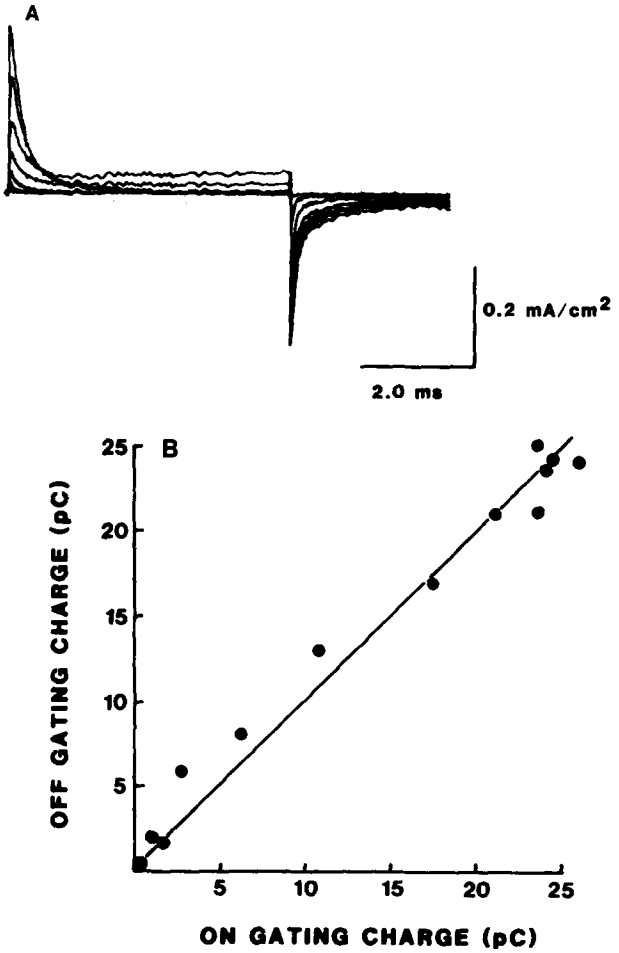

FIGURE 9. Gating currents elicited by positive test pulses from a holding potential of −150 mV. (*A*) Gating currents are illustrated for test pulses from −120 to +60 mV, at 30-mV intervals. (*B*) OFF gating charge plotted against the ON gating charge moved during the preceding test pulse. Data are from the same fiber as in *A*. Test pulses were from −135 to +60 mV, in 15-mV steps. The abscissa represents charge moved during the ON pulse from a holding potential of −150 mV. The ordinate represents the total charge moved during both fast and slow components of the OFF charge. The line is drawn through the origin with a slope of 1. A linear regression of the points yielded a slope of 1.00 and an intercept of 1.01 pC, with a correlation coefficient of .99. Muscle 50, temperature 5.2°C.

sum of two exponentials with a slow time constant of 710 μs (curve) and a fast time constant of ~48 μs (not shown). The slow component of this charge movement resembles that seen in Fig. 8, which was attributed to the recovery of gating charge from immobilization; this leads to the suggestion that considerable charge may be immobilized even at a holding potential of −90 mV. Lending support to this idea is the observation that in the same fiber, OFF gating current transients for returns from depolarizing test pulses (to

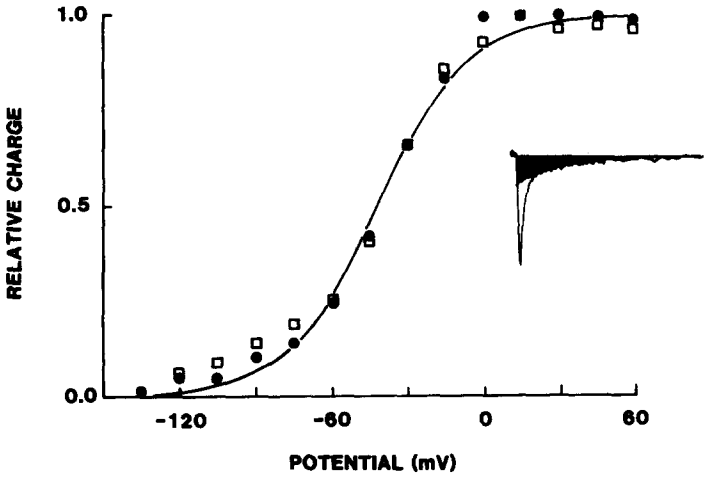

FIGURE 10. Charge vs. voltage relations. Normalized charge vs. voltage relations measured in a single fiber from two different holding potentials. Squares represent the rapidly mobile component of charge measured using hyperpolarizing and depolarizing steps from a holding potential of −90 mV. As described in the text, the slow component of charge moved by steps in the hyperpolarizing direction has the kinetics of charge recovering from immobilization. This slow charge (shaded region of inset) was estimated by fitting an exponential to the slow phase of the inward current. The remaining "rapidly mobile charge" was normalized to 0 at −150 mV and 1 at +15 mV. The filled circles represent charge measured in the same fiber using depolarizing steps from a holding potential of −150 mV. The peak charge represented by the squares is 15.8 pC, and that represented by the filled circles is 25.2 pC. The peak charge for a depolarization from −90 mV was 13.7 pC. Inset: inward charge movement in response to a step from a holding potential of −90 to −150 mV. The baseline of the current record is 4.5 ms long. Fiber 50, 5°C.

between −60 and +45 mV) to a holding potential of −150 mV could be well fitted using the same two time constants. (The amplitude of the slow component increased with both the amplitude and the duration of the preceding depolarization, as was seen in Fig. 8 at −120 mV.) In another fiber studied at 15°C, a similar current transient at −150 mV was well fitted with time constants of 250 and 18 μs, which suggests that the kinetics of both the fast and slow components are temperature dependent to about the same extent.

To obtain a measurement of the rapidly mobile charge available to move

at a holding potential of −90 mV, a single exponential was fitted to the slow component of current and the charge carried by this component (shaded area in inset of Fig. 10) was subtracted from the total inward charge movement. The resulting rapidly mobile component of charge, normalized to 0 at −150 mV and to 1.0 at its maximum value at +15 mV, is represented by the open squares in Fig. 10. The shape of this charge vs. voltage relationship is similar to that obtained in squid axons using positive and negative steps from a holding potential of −70 mV (Gilly and Armstrong, 1979). The filled circles represent the charge vs. voltage relationship determined in the same fiber over the same voltage range by holding at −150 mV and stepping only in the depolarizing direction. Both relationships have a similar shape, although the total mobile charge from the −90-mV holding potential is ~63% of the charge measured from −150 mV. The curve drawn through the points is the best visual fit of a two-state Boltzmann distribution having a valence of 1.4 and midpoint of −41 mV. Similar fits to charge vs. voltage relationships measured in nine fibers (the same group illustrated in Fig. 13) from a holding potential of −150 mV yielded an average midpoint of −35.8 ± 6.4 mV (SD) and an average valence of 1.38 ± 0.05.

In 15 fibers (13 from northern *R. pipiens* and 2 from northern *R. catesbeiana*), the maximum gating charge elicited by depolarizing steps was measured from both −90- and −150-mV holding potentials. The ratio of the charge measured from a holding potential of −90 mV to the charge measured from −150 mV in the same fiber was 0.48 ± 0.15 (mean ratio ± SD). Overall, in 34 fibers from *R. pipiens*, the maximum charge moved in depolarizations from a holding potential of −90 mV was 16.9 ± 8.7 nC/cm^2 (mean ± SD). In 17 fibers from *R. pipiens*, the maximum charge moved from a holding potential of −150 mV was 38.7 ± 20.1 nC/cm^2. Less variability and somewhat greater charge density was found in 14 fibers from *R. catesbeiana*, in which the maximum charge moved from a holding potential of −150 mV was 63.6 ± 12.7 nC/cm^2.

It is reasonable to ask whether all of the additional charge that is mobile at a holding potential of −150 mV is Na channel gating charge. Lending support to the idea that the additional charge is related to the charge that is available at a holding potential of −90 mV are the nearly identical charge vs. voltage relationships shown in Fig. 10. The effect of holding potential on ON charge movement kinetics is examined in Fig. 11. Asymmetric currents were elicited by depolarizations to five different potentials. At each potential, currents measured from a holding potential of −90 mV (dotted traces) are shown superimposed on currents measured in the same fiber from a holding potential of −150 mV (solid traces) (to facilitate the visual comparison of kinetics, the −150-mV traces have been scaled so that the peaks approximately coincide with the −90-mV traces). Except for a slight delay of 20–50 μs in the −150-mV records, the time courses are quite similar at all test potentials, which is consistent with the idea that the additional charge recruited at −150 mV is related to the charge available to move from −90 mV. This similarity in the kinetics of gating current measured at the two holding

potentials was a consistent finding and was observed in fibers studied at temperatures ranging from 5 to 15°C.

Kinetics of Gating Current

To provide a comparison with the kinetics of sodium currents, it is necessary to adopt a procedure for describing the kinetics of gating current. Collins et al. (1982*b*) found that the time integral of the gating current could be fitted

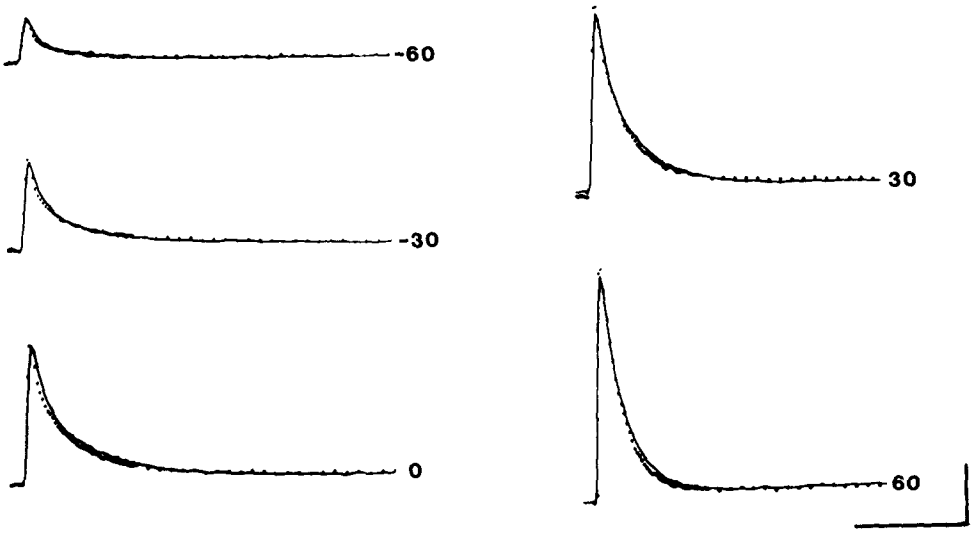

FIGURE 11. Effect of holding potential on gating current kinetics. Gating currents recorded for depolarizations to between −60 and +60 mV from a holding potential of −90 mV are shown as the dotted traces and are displayed at a single gain. Gating currents recorded in the same fiber at the same test potentials from a holding potential of −150 mV are shown as the continuous lines and are displayed at various gains so that the time courses of the currents can be compared. Except for slight delays in the currents recorded from −150-mV holding potentials, the kinetics are similar in the two sets of records. The results suggest that the additional charge moved from −150 mV is related to the charge moved from −90 mV. The vertical scale represents 0.1 mA/cm^2 for the dotted traces, and 0.13, 0.13, 0.13, 0.15, and 0.17 mA/cm^2 for the −60-, −30-, 0-, 30-, and 60-mV traces recorded from a holding potential of −150 mV.

with a single exponential. This implies that the gating current itself can also be described by a single exponential. Fig. 12 illustrates that a single-exponential decay can be fitted either to the early rapid phase or to the later slow phase of the gating current transient, but that two exponentials are required for a good fit to the entire transient. The sum of two exponentials yields equally good fits at most other potentials, although occasionally the addition of a third exponential would have provided an even better fit. The single-exponential fits obtained by Collins et al. (1982*b*) may in part be a conse-

quence of the blanking applied to the initial phase of the gating current; however, Fig. 12*d* illustrates that even without such blanking, fitting the integral of the current transient biases the fit in favor of the slower time constant. This is because the integral of the sum of exponentials weights their amplitudes in proportion to their time constants. In Fig. 12*d*, this weighting resulted in a reasonable fit of a single exponential with a time constant nearly identical to that of the slower exponential fitted to the gating current transient. However, at other voltages, the weighting yielded approximately single-exponential fits with time constants intermediate between the fast and slow time constants. For comparison with ionic current kinetics, gating

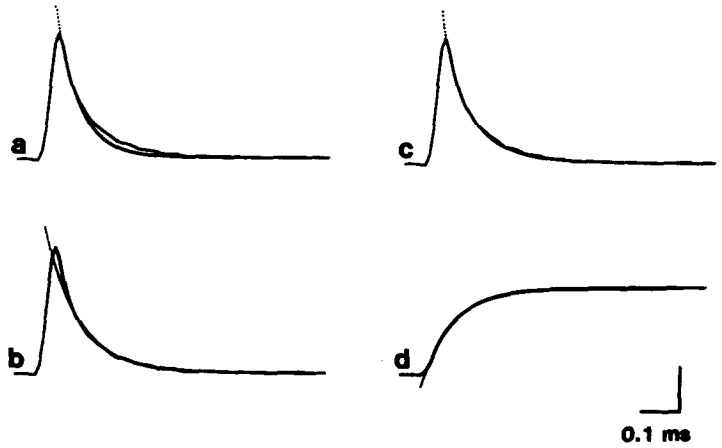

FIGURE 12. Fitting the kinetics of gating current. Frames *a–c* show the same gating current transient, elicited by a step to +30 mV. (*a*) Superimposed on the gating current record is a single-exponential decay fitted by eye to the fast phase (time constant 48 μs) of the current transient. (*b*) A single exponential is fitted to the slow phase of the gating current decay (time constant 83 μs). (*c*) The sum of two exponentials (20 and 83 μs) provides an excellent fit to virtually the entire falling phase of the gating current. (*d*) The integral of the current transient appears well fitted by a single exponential of 83 μs. Vertical calibration: 0.2 mA/cm^2 for the current transient and 13 pC for the integral.

currents were fitted with the sum of two exponentials as shown in Fig. 12*c*, since that method was both simple and well constrained.

In Fig. 13 the voltage dependence of the slower of the two time constants (τ_g) obtained in fits to gating currents is compared with the values of τ_m obtained in fits to Na currents recorded in the same group of fibers. The magnitude and voltage dependence of τ_g and τ_m are similar but not identical. In the cold, τ_m and τ_g are both slowed to a similar extent. Although it was not as precisely determined, the fast time constants obtained in the fits were also slower in the cold, ranging from 40 to 100 μs in the 4–5°C experiments and from 20 to 40 μs in the 12–15°C experiments.

The gating current and activation time constants shown in Fig. 13 partially

overlap at positive potentials, but differ substantially below about −15 mV. Fig. 14 demonstrates that this difference extends to currents measured at still more negative potentials. The figure shows the responses of a muscle fiber elicited by returning to −90 mV from a 3-ms prepulse to 0 mV. The same fiber was bathed first in K-free Na Ringer and then in gating current solution. In Ringer, the prepulse opens Na channels and the subsequent steps to −90 mV causes a large inward current tail as channels quickly close. This

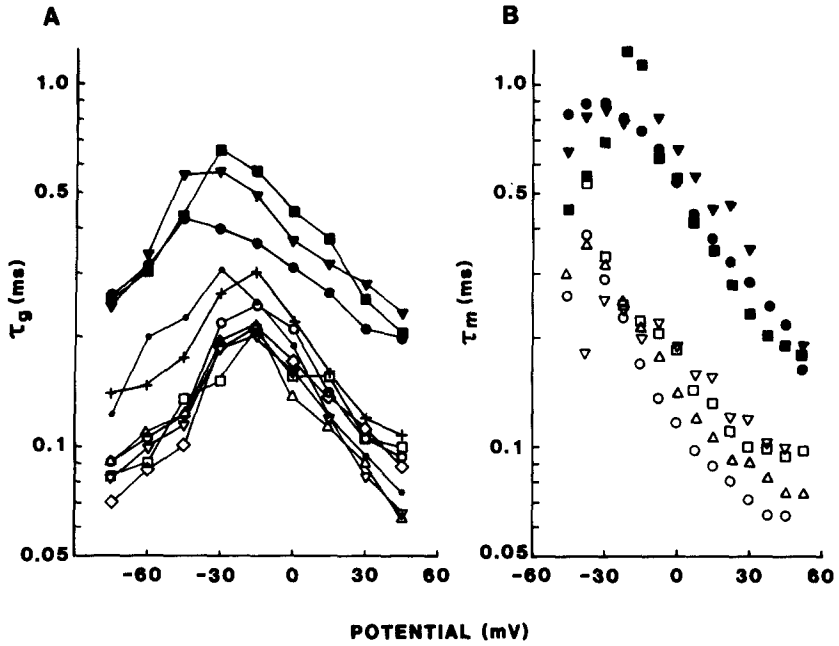

FIGURE 13. Kinetics of gating and ionic currents. (*A*) The slower of the two time constants, τ_g, obtained as illustrated in Fig. 12*c*, is plotted against voltage for 10 fibers. Solid symbols represent fibers studied at 5°C. The other fibers were studied at 12–15°C. (*B*) τ_m determined by least-squares fits of the expression $[1 - \exp(-t/\tau_m)]^3[\exp(-t/\tau_h)]$ to ionic currents measured in the same group of fibers as in *A*. Individual fibers are represented by the same symbol in *A* and *B*. (Ionic currents were not recorded under the same conditions in three of the fibers represented in *A*.) Holding potential −150 mV. Ionic currents were measured in K-free Na Ringer.

current tail and the corresponding OFF gating current are shown at different gains so that their time courses can be compared. As in the squid axon, at −90 mV the gating current declines ~1.5 times more slowly than the corresponding ionic current (Armstrong and Bezanilla, 1974; Armstrong, 1981). By contrast, the Hodgkin and Huxley (1952) model predicts that the gating current would decline three times more slowly than the ionic current (Armstrong, 1981).

DISCUSSION

The fast asymmetric charge movements reported here share many of the characteristics of putative sodium channel gating currents previously reported in nerve and muscle. The charge movement saturates below about −120 mV and above about +30 mV. The OFF charge upon returning to −150 mV is equal to the ON charge moved during the preceding depolarization, which supports the idea that the charge is confined to the membrane. At a holding potential of −90 mV, the OFF charge is generally smaller than the ON charge during the preceding depolarization, a process that is also observed in axons and is called charge immobilization. As in nerve (Armstrong and Bezanilla, 1977; Nonner, 1980), this immobilization parallels the rate of inactivation of sodium currents measured in the same fiber, and is therefore consistent with the hypothesis that immobilization of charge reflects the inactivation of Na channels.

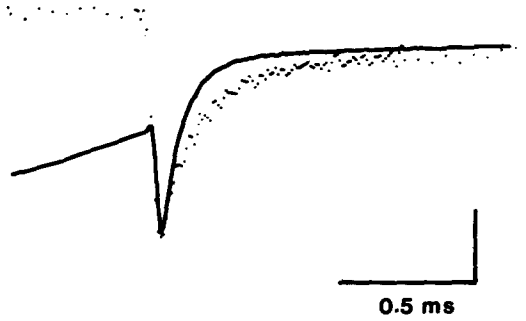

FIGURE 14. Sodium tail current and OFF gating current at −90 mV. For comparison, the gating current (dotted trace) was scaled to make the peaks approximately coincide. The current transients could be approximated by single exponentials with time constants of 98 μs for the ionic current tail and 158 μs for the OFF gating current. Vertical scale represents 1 mA/cm^2 of ionic current and 0.037 mA/cm^2 of gating current. Muscle 94, temperature 4.2°C.

In the average fiber the charge vs. voltage relationship can be reasonably well fitted by a two-state Boltzmann distribution with a valence of 1.38 and a midpoint of about −36 mV, values close to those previously reported in muscle (Collins et al., 1982*b*). However, it is typically observed that between −120 and −90 mV the measured charge consistently lies above the best-fitting Boltzmann curve. It seems likely, therefore, that the two-state model is too simple to accurately describe the gating charge distribution. A similar "bump" has been observed in charge vs. voltage relations measured in squid axons (Bezanilla and Armstrong, 1975; Armstrong and Gilly, 1979; Bezanilla et al., 1982).

The time constant of the slower phase of gating current considerably overlaps the value of τ_m determined from fits to ionic currents, particularly at potentials above 0 mV. Within the population of fibers studied, it is

possible to find some pairs of gating and ionic current records from individual fibers that show relative agreement in these time constants and therefore seem to support the Hodgkin and Huxley (1952) model of Na channel kinetics. However, in other records from the same fibers, the two time constants are rather different, especially at relatively negative potentials and for tail/OFF gating currents (Fig. 14), where the disagreement is considerable.

Slow Movements of Gating Charge

The idea that the gating current is capacitative requires that the charge which moves during the ON transient must eventually return during the OFF transient. Thus, it has been hypothesized that charge immobilization occurs because its return at moderate holding potentials is simply too slow to be resolved (Armstrong and Bezanilla, 1977). In support of this hypothesis, Armstrong and Bezanilla (1977) demonstrated that in the squid axon, OFF charge at hyperpolarized holding potentials contained both fast and slow components. However, they found that the total OFF charge at −140 mV was constant, independent of prepulse duration, and approximately equal to the ON charge moved during the prepulse. On this basis they hypothesized that the slow component of OFF gating current at hyperpolarized potentials represents the return charge "immobilized" during the prepulse. The present results support this interpretation of the slow OFF charge movement in frog muscle. Increasing the ON pulse duration and increasing the ON pulse amplitude, both of which increase charge immobilization, increases the proportion of the slow component of OFF charge movement (Fig. 8). In addition, as demonstrated by Fig. 12, the total OFF charge measured at −150 mV is equal to the ON charge moved during the prepulse. This result supports the notion that the charge is capacitative and it is consistent with the hypothesis that charge which was immobilized during the prepulse nevertheless returns quickly enough to be measured in an OFF step to −150 mV.

Collins et al. (1982*b*) also observed fast and slow phases of OFF charge movement at −140 mV. They reported that the magnitude of the slow component was not affected by ON pulse amplitude and found that ON charge equaled OFF charge only when the slow component was subtracted from the record. These apparent discrepancies between their results and mine are resolved by comparing the kinetics of OFF charge movements. The "fast" component reported by Collins et al. (1982*b*) had a time constant of 150–300 μs at −140 mV and 19°C, which is similar to the 250-μs time constant of the "slow" component I saw at −150 mV and 15°C. A faster component, which in my experiments had a time constant of the order of 20 μs at −150 mV and 15°C, was not seen in the records shown in Fig. 9 of Collins et al. This appears to be due to the relatively long interval blanked from the beginning of their records (estimated from measurement of their Fig. 9 to be ~70 μs). In the experiment illustrated in my Fig. 9, the bulk of the OFF charge moves during what I have called the "slow" component, which appears to be identical to what Collins et al. have called the "fast" component. Apparently, the quantity of charge lost during the blanking interval was

approximately the same in the ON and OFF charge movements that Collins et al. found to be equal.

The slower component of OFF charge movement reported by Collins et al. was not typically seen in my experiments. This may have been due to the presence of 5 mM Cs and the absence of K in my gating current solution, which appeared to linearize the leakage currents and may have eliminated a small ionic component of the OFF current. Alternatively, Collins et al. generally worked at a higher temperature (19°C as compared with 5–12°C in the present experiments), and it is possible that their slow component of OFF current was present in my records but was too slow to be detected.

Charge Movement at Hyperpolarized Potentials

A variety of possibilities have been suggested for the function of gating charge movement observed in nerve over the hyperpolarizing potential range (below about −80 mV). One possibility is that it may be related to the delay in sodium current activation caused by hyperpolarization (Armstrong and Bezanilla, 1974). It has also been suggested that the charge which moves over hyperpolarizing potentials may be of "unknown function" and is possibly unrelated to sodium channel gating (Armstrong, 1981). One reason for suggesting this second possibility is that this potential range is far from the range over which Na channels are activated. However, the charge that moves for hyperpolarizing steps from −90 mV is presumably a part of the charge that moves during positive steps from −150 mV. If this charge were unrelated to Na channel gating, it might be expected to have a different charge vs. voltage relationship and different kinetics. Instead, Fig. 10 demonstrates that the rapidly mobile component of charge available to move from a holding potential of −90 mV has a charge vs. voltage relationship similar to that measured from −150 mV, and Fig. 11 shows that the kinetics of gating currents measured from holding potentials of −90 and −150 mV are quite similar. I know of no reports of the effect that holding for long periods of time at −150 mV has on the magnitude of gating current in axons. Meves (1974) reported a 40% increase in gating charge in a squid axon as a consequence of changing the holding potential from −88 to −101 mV. However, in this early work on gating currents, the control pulse was a hyperpolarizing step from the holding potential, and therefore the control currents at the two holding potentials would have contained different amounts of asymmetric charge, making a quantitative comparison difficult.

Some of the charge that moves over the hyperpolarized voltage range should be accounted for by the process of "removing inactivation," which in muscle involves both fast and slow processes. For instance, when a fiber held at −90 mV is stepped to −150 mV for a few milliseconds, the peak sodium current elicited by a depolarization to 0 mV is increased by ~15% relative to the −90-mV control. Holding a muscle fiber at −150 mV causes a larger increase in peak current, ~30% in the first minute or two (about half of which can be accounted for by the removal of fast inactivation). A further increase of 10–15% occurs over the course of about the next 10 min (D. T.

Campbell, unpublished results). These slow increases in peak conductance are due to the reversal of the so-called "slow" and "ultra-slow" inactivation (Fox, 1976; Brismar, 1977; Collins et al., 1982*a*), and together with removal of fast inactivation, they result in a total increase in peak conductance of 40–45% for a change of holding potential from −90 to −150 mV. This relative increase in Na conductance is only about half of the increase observed in gating charge upon holding at −150 mV. A discrepancy between recovery of charge and reversal of inactivation has also been described in the squid axon by Bezanilla et al. (1982). The membrane potential was first held at 0 mV for 2–3 min, totally inactivating the Na conductance and immobilizing the bulk of the gating charge. From this condition, a hyperpolarizing pulse to −160 mV caused virtually all of the immobilized charge to return in 1–2 ms, with almost no recovery of Na conductance (Bezanilla et al., 1982). By contrast, hyperpolarizing to −130 mV for 100 ms or to −170 mV for 50 ms permitted only a small fraction of the Na conductance to recover. The authors concluded that long-term inactivation may cause the channel to become unable to open, without preventing the gating machinery from moving and being detected as gating current. This result suggests that channels that are nonconducting can nevertheless contribute their charge to the measured gating current. Thus, it is possible that in the present experiments, holding at −150 mV recruits Na channels whose charge can move but cannot conduct.

I wish to thank Dr. K. Beam for helpful discussions during the course of this work, and Drs. Beam and R. Hahin for commenting on the manuscript. I thank Ms. M. Boyken for assistance in preparing the manuscript.

Supported by the Muscular Dystrophy Association of America and NS 15400 from the U. S. Public Health Service.

Received for publication 29 July 1982 and in revised form 5 July 1983.

REFERENCES

Adrian, R. H., and L. D. Peachey. 1973. Reconstruction of the action potential of frog sartorius muscle. *J. Physiol. (Lond.)*. 235:103–131.

Almers, W., R. Fink, and N. Shepherd. 1982. Lateral distribution of ionic channels in the cell membrane of skeletal muscle. *In* Disorders of the Motor Unit. D. L. Schotland, editor. John Wiley & Sons, New York. 349–365.

Armstrong, C. M. 1981. Sodium channels and gating currents. *Physiol. Rev.* 61:644–683.

Armstrong, C. M., and F. Bezanilla. 1974. Charge movement associated with the opening and closing of the activation gates of the Na channels. *J. Gen. Physiol.* 63:533–552.

Armstrong, C. M., and F. Bezanilla. 1977. Inactivation of the sodium channel. II. Gating current experiments. *J. Gen. Physiol.* 70:567–590.

Armstrong, C. M., and W. F. Gilly. 1979. Fast and slow steps in the activation of sodium channels. *J. Gen. Physiol.* 74:691–711.

Armstrong, C. M., and B. Hille. 1972. The inner quaternary ammonium ion receptor in potassium channels of the node of Ranvier. *J. Gen. Physiol.* 59:388–400.

Bezanilla, F., and C. M. Armstrong. 1975. Properties of the sodium channel gating current. *Cold Spring Harbor Symp. Quant. Biol.* 40:297–304.

Bezanilla, F., R. E. Taylor, and J. M. Fernandez. 1982. Distribution and kinetics of membrane dielectric polarization. I. Long-term inactivation of gating currents. *J. Gen. Physiol.* 79:21–40.

Brismar, T. 1977. Slow mechanism for sodium permeability inactivation in myelinated nerve fibre of *Xenopus laevis*. *J. Physiol.* (*Lond.*). 270:283–297.

Campbell, D. T. 1981. Sodium channel gating currents in frog skeletal muscle. *Biophys. J.* 33:282*a*. (Abstr.)

Campbell, D. T., and R. Hahin. 1983. Functional disruption of the T-system of cut muscle fibers bathed in solutions of normal tonicity. *Biophys. J.* 41:177*a*. (Abstr.)

Chandler, W. K., R. F. Rakowski, and M. F. Schneider. 1976. A non-linear voltage dependent charge movement in frog skeletal muscle. *J. Physiol.* (*Lond.*). 254:245–283.

Collins, C. A., E. Rojas, and B. Suarez-Isla. 1982*a*. Activation and inactivation characteristics of the sodium permeability in muscle fibers from *Rana temporaria*. *J. Physiol.* (*Lond.*). 324:297–318.

Collins, C. A., E. Rojas, and B. Suarez-Isla. 1982*b*. Fast charge movements in skeletal muscle fibres from *Rana temporaria*. *J. Physiol.* (*Lond.*). 324:319–345.

Dodge, F., and B. Frankenhaeuser. 1959. Sodium currents in the myelinated nerve of *Xenopus laevis* investigated with the voltage clamp technique. *J. Physiol.* (*Lond.*). 148:188–200.

Fox, J. M. 1976. Ultra-slow inactivation of the ionic currents through the membrane of myelinated nerve. *Biochim. Biophys. Acta.* 426:232–244.

Hahin, R., and D. T. Campbell. 1982. Low pH modulates Na channel gating currents in frog muscle. *Biophys. J.* 37(2, Pt. 2): 315*a*. (Abstr.)

Hamming, R. W. 1977. Digital Filters. Prentice-Hall, Inc., Englewood Cliffs, NJ. 226 pp.

Hille, B., and D. T. Campbell. 1976. An improved vaseline-gap voltage clamp for skeletal muscle fibers. *J. Gen. Physiol.* 69:265–293.

Hodgkin, A. L., and A. F. Huxley. 1952. A quantitative description of membrane current and its application to conduction and excitation in nerve. *J. Physiol.* (*Lond.*). 117:500–544.

Horowicz, P., and M. F. Schneider. 1981. Membrane charge movement in contracting and non-contracting skeletal muscle fibers. *J. Physiol.* (*Lond.*). 314:565–593.

Meves, H. 1974. The effect of holding potential on the asymmetry currents in squid giant axons. *J. Physiol.* (*Lond.*). 254:787–801.

Nonner, W. 1980. Relations between the inactivation of sodium channels and the immobilization of gating charge in frog myelinated nerve. *J. Physiol.* (*Lond.*). 299:573–603.

Rojas, E., and B. Suarez-Isla. 1980. Charge displacement associated with the activation of the sodium conductance in frog skeletal muscle fibres. *J. Physiol.* (*Lond.*). 301:46–47p.

Schneider, M. F., and W. K. Chandler. 1973. Voltage dependent charge movement in skeletal muscle: a possible step in excitation contraction coupling. *Nature* (*Lond.*). 242:244–246.

Sizto, N. L. 1982. Sodium gating current and sodium current in frog twitch muscle fibers. *Biophys. J.* 37:69*a*. (Abstr.)

Vergara, J., and M. Cahalan. 1978. Charge movements in a cut skeletal muscle fiber. *Biophys. J.* 21:167*a*. (Abstr.)